Journal of Hydroscience and Hydraulic Engineering
Vol. 15, No. 1, June, 1997, 35-45

APPLICATION OF STORMWATER RUNOFF MODELS TO AN URBAN LOWLAND CATCHMENT

By

Kazumasa Fujimura

Rsearch Associate, Department of Civil Engineering,
Tokyo Metropolitan University,
1-1 Minamiohsawa, Hachioji-shi, Tokyo 192-03, Japan

and

Yosihisa Ando

Professor, Department of Civil Engineering,
Tokyo Metropolitan University,
1-1 Minamiohsawa, Hachioji-shi, Tokyo 192-03, Japan

SYNOPSIS

In this study three stormwater runoff models based on an effective rainfall model and a physically based runoff model are applied to an urban lowland catchment in a pump drainage area. The final infiltration capacities which were measured in a field for each type of land use using a rainfall simulator are used in the effective rainfall model. Kinematic wave equations are chosen for calculation of surface flow. On the other hand, dynamic wave, diffusion wave and kinematic wave equations are used to calculate channel flow because the channel slopes are considered to be moderate.

We conclude that the method using diffusion wave equations is the most appropriate runoff model after comparison with the method using kinematic wave and dynamic wave equations for this urban lowland catchment.

INTRODUCTION

There are many urban areas located in lowlands. Rainwater in these areas should be drained off immediately using pumps. In order to operate pumping stations and to manage drainage systems efficiently, it is important to develop models for stormwater runoff and apply them to practical catchments in order to prevent and reduce the disaster of urban floods.

Physical hydrological models require few parameters and little calibrations because they use physical equations which are controlled by the gravity effect, and they are appropriate for a variety of catchment conditions. However, such models require numerical solution techniques and computing capability. The kinematic wave model has been successfully used as a hydrological model for stormwater runoff simulations since Wooding (11) (12) introduced the V-shaped model for surface and channel flows. Ponce et al. (7) indicated that the diffusion model is applicable to a wider range of bed slopes and wave periods than the kinematic model. Kinosita (6) remarked on the general criteria for choosing physical equations for an unsteady flow analysis with respect to channel slopes, namely, that the kinematic wave equations are appropriate in the case of slopes greater than 1/1000, the diffusion wave equations are

appropriate for slopes greater than 1/3000 and the dynamic wave equations are appropriate for slopes less than 1/3000. It is said that the kinematic wave model is limited to slopes that are moderate, whereas the dynamic wave and diffusion wave models are appropriate for analyzing flow on moderate slopes, such as those found in lowland catchments, by considering the downstream boundary condition.

We compare the accuracy of the stormwater runoff models using the dynamic wave, diffusion wave and kinematic wave equations for an urban lowland catchment. We have selected an effective rainfall model proposed by Ando et al. (4) for the purpose of estimating excess rainfall for areas of various types of land use in an urban catchment. The model concept consists of the initial losses and final infiltration capacities for each type of land use. Ando et al. (3) have also simulated the runoff hydrograph of urban upland catchments using the effective rainfall model and the kinematic wave runoff model, and have indicated good applicability.

In this study the model in which the dynamic wave equations are used to calculate channel flow is simply called the 'dynamic wave method'. Similarly, the models in which the diffusion wave and kinematic wave equations are used are called the 'diffusion wave method' and the 'kinematic wave method', respectively.

STUDY CATCHMENT

The Shinkomatsu River catchment used in this study is within the Tokyo lowland area which is a typical lowland area in Japan. The catchment area is 2.04 km^2 and is situated between the Ara River and the Kyu-Naka River, as shown in Fig. 1. The distance from the sea, Tokyo Bay, is about 7 km and the elevation of most of the area is less than 0 m above sea level, and so the catchment is surrounded by levees and revetments. The rainwater which flows through the main channels and branch channels must be completely drained to the Kyu-Naka River by the pumping station which is indicated as P in Fig. 1.

The percentages of land use given in Table 1 were obtained by superimposing a 50 m mesh on

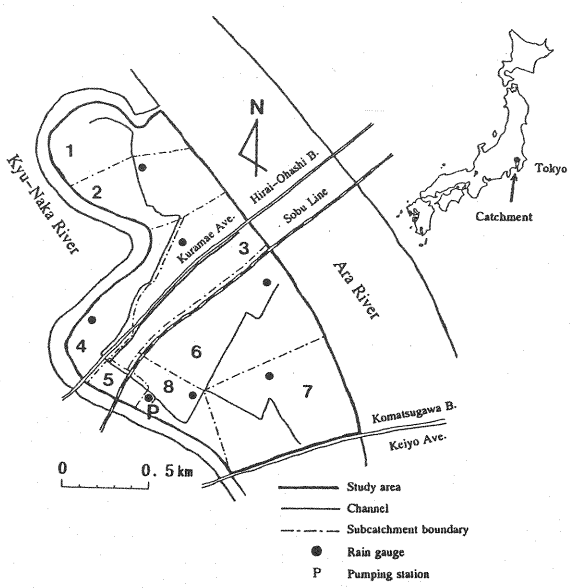

Fig.1 Map of the Shinkomatsu River catchment

Table 1 The percentages of areas of various land uses and the measured final infiltration capacities

Land uses	Sports grounds	Private gardens	Roads, others
Percentages of areas (%)	6.4	33.2	60.4
Final infiltration capacities (mm/hr)	2.3	5.1	0

a 1:2500 scale map from 1988 and comparing it with an aerial photograph. The catchment is classified as an urban area because the percentage of impervious area, which includes roads, parking lots and roofs, is 60.4%. The other percentages of land use are 6.4% for sports ground and 3.2% for private gardens.

Automatic tipping-bucket rain gauges, which are indicated by black points in Fig. 1 are installed at seven locations in the catchment area. Runoff data are obtained from the balance between the amounts of inflow to the pumping station, water in the reservoir and discharge at the pumping station. Both rainfall and runoff data are recorded at 1 minute intervals.

EFFECTIVE RAINFALL MODEL

For the purposes of estimating excess rainfall in areas with various land uses in an urban catchment, we adopted the effective rainfall model presented by Ando et al. (4). The catchment is divided into impervious and pervious areas in this model, as shown in Fig. 2.

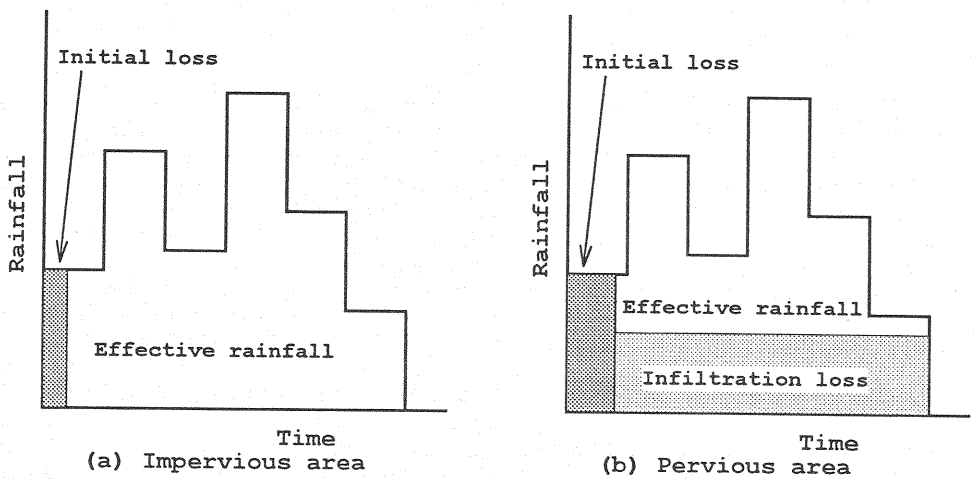

Fig. 2 Effective rainfall models for impervious area (a) and pervious area (b) (from Ando et al. 1986)

For impervious areas, the initial loss of rainfall can be defined as surface ponding and is given by

$$Re_{imp}(t) = 0 \quad \text{if} \quad \sum R(t) \leq L_{imp}$$

$$Re_{imp}(t) = R(t) \times \frac{60}{DT} \quad \text{if} \quad \sum R(t) > L_{imp}$$

where L_{imp} is the initial loss of rainfall (mm), R(t) is the rainfall at time t (mm), DT is time interval (min) and $Re_{imp}(t)$ is the effective rainfall rate (mm/hr) in one time interval. Although Tholin and Keifer (10) assumed the rate of initial loss in an impervious area to be 1.6 mm, Yamaguchi et al. (13) used 2 mm in their flood runoff analysis using the RRL method for urban river catchments, as did Ando et al. (2) for their investigation of the Tama New Town area in Tokyo. We also used a value of 2 mm.

For pervious areas, the effective rainfall can be estimated from the initial loss and the final infiltration capacity and is given by

$$Re_p(k, t) = 0 \quad \text{if} \quad \sum R(t) \leq L(k)$$

$$\left.\begin{aligned} Re_p(k, t) &= 0 && (\ R(t) \leq IC(k)\ ) \\ Re_p(k, t) &= R(t) \times \frac{60}{DT} - IC(k) && (\ R(t) > IC(k)\ ) \end{aligned}\right\} \quad \text{if} \quad \sum R(t) > L(k)$$

where L(k) is the initial loss of rainfall (mm), $Re_p(k,t)$ is the effective rainfall rate (mm/hr) and IC(k) is the final infiltration rate (mm/hr) in one time interval, for the (k)th pervious area. For the two types of land use in the present catchment, sports grounds and private gardens, the final infiltration capacities were measured using a rainfall simulator by Ando (1). The median values are given as 2.3 mm/hr for sports grounds and 5.1 mm/hr for private gardens in Table 1. It is difficult to predict the initial loss in a pervious area, because it depends on such factors as antecedent rainfall, soil moisture, humidity and temperature, and so the optimum values of initial loss are obtained from calibrations.

RUNOFF MODEL

Modeling of the catchment

For cases in which the stormwater runoff process is analyzed using physical equations, it is valid to represent the catchment by a combination of surface and channel flow models, which was proposed by Wooding (11) (12) as the V-shaped model. Although the course of rainwater flow in a catchment cannot be routed exactly in the case of a lowland area, the present catchment was divided into eight subcatchments subject to the flow course of the main channels, as shown in Fig. 3.

The slopes of surfaces and channels are shown in Table 2, in which the slopes of surfaces are between 0.12% and 6.32% with an average of 0.839%, and those of channels are between 0.03% and 0.68% with an average of 0.204%. Half of the channel slopes are less than 0.1% (1/1000), which is a characteristic feature of a lowland. The kinematic wave equations are selected for surface flow calculation because the surface slopes are not moderate, whereas the dynamic wave, diffusion wave and kinematic wave equations are used for the channel flow calculation, because the slopes can be considered moderate rather than steep.

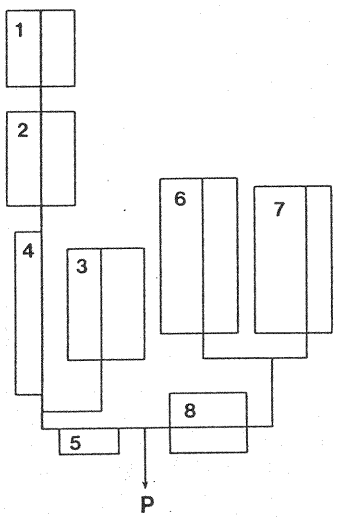

Fig. 3 Schematic model of the Shinkomatsu River catchment

Tabel 2 The surface and channel slopes

Subcatchment	Surface (%)	Channel (%)
1-R	0.44	0.68
1-L	0.40	-
2-R	1.08	0.099
2-L	0.30	-
3-R	0.22	0.150
3-L	0.14	-
4-R	6.32	0.063
5-R	0.48	0.030
6-R	0.29	0.390
6-L	0.26	-
7-R	0.27	0.180
7-L	0.12	-
8-R	0.35	0.043
8-L	1.08	-
Average	0.839	0.204

Surface flow model

The kinematic wave equations based on the Manning formula are selected for the surface flow analysis, and can be written as

$$q = \frac{1}{N} h^{\frac{5}{3}} s^{\frac{1}{2}} \tag{1}$$

$$\frac{\partial h}{\partial t} + \frac{\partial q}{\partial x} = r \tag{2}$$

where N is the equivalent roughness, h and q are the depth and the discharge of rainwater flow on the surface, respectively, s is the slope of the surface, r is the effective rainfall, Δt is the time interval and Δx is the distance interval. The above equations are solved by means of a finite difference scheme in which the time differential terms are treated in the forward difference scheme and the distance differential terms are treated in the backward differential scheme.

Sueishi (9) demonstrated the equivalent roughness (N) for the surface flow equations to be the surface condition of a catchment, and he used an N of 0.3 ($sec/m^{1/3}$) in the runoff simulation of the Daido River catchment in a mountain area in Shiga, Japan. Although typical values of equivalent roughness were presented by Kadoya (5) as N=0.01 - 0.04 ($sec/m^{1/3}$) for urban areas, we use a value of N=0.008 ($sec/m^{1/3}$) for the present catchment, which was used for the urban upland areas in the study by Ando et al. (3).

The initial values for the depth h and the discharge q are given as 0. The upstream conditions for the depth h and the discharge q are also given as 0.

Channel flow model

Dynamic wave method

One of the methods used here for analyzing the channel flow is the dynamic wave method. The equations are complete Saint Venant equations and are written as

$$\frac{1}{g}\frac{\partial u}{\partial t} + \frac{u}{g}\frac{\partial u}{\partial X} + \frac{\partial H}{\partial X} = S - \frac{n^2 u|u|}{R^{\frac{4}{3}}} \tag{3}$$

$$\frac{\partial A}{\partial t} + \frac{\partial Q}{\partial X} = q \tag{4}$$

where g is the gravity constant, A is the cross-sectional area, Q is the discharge of channel flow, q is the lateral inflow, u is the average flow velocity given by Q/A, H is the depth of the channel, R is the hydraulic radius, n is Manning's roughness coefficient and X is the distance.

Since the phenomenon of stormwater runoff can be considered as intensive unsteady flow, the two-step Lax-Wendroff scheme, a finite difference scheme, is chosen to solve the dynamic wave equations. The two-step Lax-Wendroff scheme, which is a variant of the Lax-Wendroff scheme, is well suited for the Eulerian equations in the case of slab symmetry such as the jump condition because it is described as the conservation-low form (Richtmyer and Morton, (8)).

Manning's n for the channels are taken as n=0.02 for rectangular channel flow and n=0.015 for conduit pipe flow, as are commonly used. The same values of Manning's n are used for the channel flow calculations by the diffusion wave and kinematic wave methods in the following section. The initial conditions of the cross-sectional area A and the discharge Q are obtained from the uniform flow for normal discharge at the pump station on a day without rain. The downstream boundary condition at the end node, the discharge Q and the cross-sectional area A, are obtained from the calculated Q and A at one step before end node. The upstream boundary condition for Q and A at first node is obtained from the downstream boundary condition of the upstream channel. The time step is selected as Δt=0.5 sec and the distance step is selected as Δx=10 m for the surface flow calculations and ΔX=10 m for the channel flow calculations.

Diffusion wave method

The diffusion wave equations are an approximation of the Saint Venant equations and are written as

$$Q = \frac{1}{n} A R^{\frac{2}{3}} \left(S - \frac{\partial H}{\partial X} \right)^{\frac{1}{2}} \tag{5}$$

$$\frac{\partial A}{\partial t} + \frac{\partial Q}{\partial X} = q \tag{6}$$

To solve the diffusion wave equations by means of a finite difference scheme, the time differential terms are treated in the forward difference scheme and the distance differential terms are treated in the backward difference scheme.

The initial condition for the discharge Q is given as 0. The upstream and downstream boundary conditions for the discharge Q and the cross-sectional area A are the same as those used in the dynamic wave method calculation. The time step is selected as Δt=1.0 sec and the distance step is selected as Δx=10 m for the surface flow and ΔX=30 m for the channel flow calculations.

Kinematic wave method

The kinematic wave equations are also an approximation of the Saint Venant equations. The momentum equation is divided into two types in the case of this catchment. Manning's equation is used for rectangular channel flow and an exponential functional equation is used for circular pipe flow, because the relationship between water depth and discharge of circular pipe flow cannot easily be expressed in Manning's equation. The parameters in an exponential functional equation are determined by Manning's equation. The momentum and continuity equations for the kinematic wave method can be written as

$$Q = K A^{P} \text{ (for circular pipe flow)} \tag{7}$$

$$Q = \frac{1}{n} A R^{\frac{2}{3}} S^{\frac{1}{2}} \text{ (for rectangular channel flow)} \tag{8}$$

$$\frac{\partial A}{\partial t} + \frac{\partial Q}{\partial X} = q \tag{9}$$

where K and P are the channel flow parameters for circular pipe flow.

The initial conditions for the discharge Q and the cross-sectional

area A are both given as 0. The upstream boundary conditions for Q and A at the first node are obtained from the downstream boundary conditions of the upstream channel. The time step is selected as Δt=4.0 sec and the distance step is selected as Δx=10 m for the surface flow and ΔX=40 m for the channel flow calculations. A finite difference scheme is chosen to solve the above equations as same as the kinematic wave equations (1) and (2) for the surface flow.

RESULTS

Analyses using these methods were performed using a workstation with a capability of 28.5 million instructions per second (MIPS) for fourteen rainfall events in 1991. The specifications of these events and the initial losses used in the calculations are given in Table 3.

Typical examples of the observed hydrographs and simulated hydrographs obtained using these three methods are presented in Fig. 4. The simulated hydrograph obtained using the kinematic wave method is overestimated in the recession region, while the simulated hydrographs obtained using the dynamic wave and diffusion wave methods agree more closely with the observed hydrographs in both the rising and recession regions. To compare the performance of the three methods, the computer time, the relative errors in peak runoff (REP) and total runoff (RET), and the mean value of relative errors for one-minute intervals (MRE) are used.

Table 3 Rainfall events in 1991 and initial losses

No.	Date	Total rainfall (mm)	Total runoff (mm)	Peak runoff (mm/hr)	Initial loss (mm)
1	23 June	33.8	15.0	10.0	10
2	5 July	31.7	12.6	12.5	5
3	1 Aug.	11.8	5.0	16.4	1
4	12 Aug.	64.3	29.2	13.3	50
5	20 Aug.	62.9	30.3	12.2	10
6	30 Aug.	27.2	11.8	10.0	10
7	8 Sep.	75.8	40.8	29.5	55
8	14 Sep.	24.4	13.5	9.9	10
9	18 Sep.	204.6	135.2	39.6	50
10	30 Sep.	93.9	43.2	9.3	10
11	11 Oct.	108.9	82.8	11.9	10
12	27 Oct.	40.8	19.8	9.0	10
13	8 Nov.	44.6	20.0	16.3	10
14	28 Nov.	81.5	38.7	13.8	10

The REP is given by

$$REP(\%) = \frac{QPC - QPO}{QPO} \times 100 \qquad (10)$$

where QPC is the calculated peak discharge and QPO is the observed peak discharge.

The RET is given by

$$RET(\%) = \frac{\sum QC(t) - \sum QO(t)}{\sum QO(t)} \times 100 \qquad (11)$$

where QC(t) is the calculated discharge and QO(t) is the observed discharge at time t.

The MRE is given by

$$MRE(\%) = \frac{1}{NM} \sum \frac{\left| QC(t) - QO(t) \right|}{QO(t)} \times 100 \qquad (12)$$

where NM is the number of data.

Table 4 gives a summary of these results and Table 5 gives a comparison of the computer time required for these methods. The following are noted.

(1) The average values of REP obtained using the dynamic wave and diffusion wave methods were 18.0% and 12.3% respectively, whereas that obtained using the kinematic wave method was significantly higher at 37.6%.

(2) The average values of RET obtained using the dynamic wave and diffusion wave methods were similar, 32.4% and 29.9%, respectively. However, the value obtained using the kinematic wave method was 66.9%.

(3) The average values of MRE obtained using the dynamic wave and diffusion wave methods were 32.4% and 26.1%, respectively, whereas the kinematic wave method gave a higher value of 57.5%.

(4) The computer time required for analyzing hourly data for the dynamic wave method was 4 min. 30 sec. and these for the diffusion wave and kinematic wave methods were 1 min. 30 sec. and 7 sec. respectively.

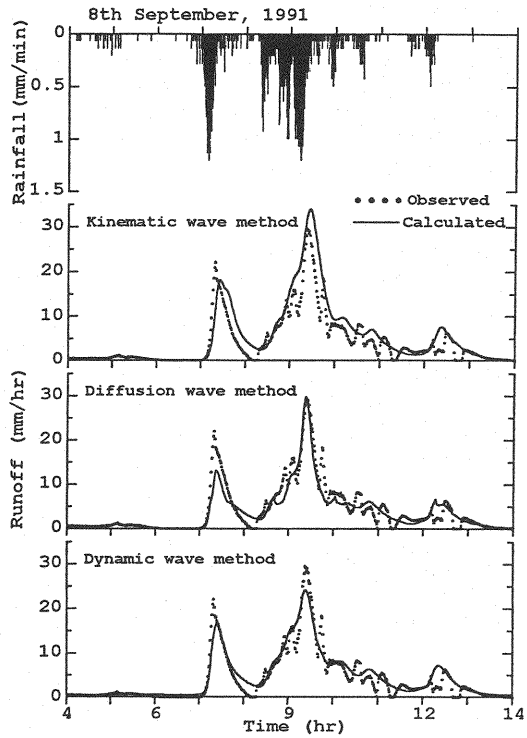

Fig. 4 Results of the observed and simulated hydrographs of the three methods

Table 4 Results for RET, REP and MER value from the three methods

No.	Date	Dynamic wave method					Diffusion wave method					Kinematic wave method				
		Σ QC (mm)	RET (%)	QPC (mm/h)	REP (%)	MER (%)	Σ QC (mm)	RET (%)	QPC (mm/h)	REP (%)	MER (%)	Σ QC (mm)	RET (%)	QPC (mm/h)	REP (%)	MER (%)
1	23 June	21.4	43.5	11.8	18.0	29.8	20.4	36.1	9.5	-5.1	19.2	27.0	80.8	15.0	50.0	59.3
2	5 July	20.8	65.2	13.0	4.0	27.1	21.3	69.1	11.9	-4.5	23.0	26.4	110.5	18.1	44.8	49.9
3	1 Aug.	7.5	49.9	15.5	-5.5	50.1	6.6	31.6	13.5	-17.7	33.2	9.5	90.1	18.4	12.2	96.8
4	12 Aug.	33.2	14.0	16.1	21.1	34.6	28.3	-2.9	14.0	5.0	23.7	44.4	52.3	21.8	63.9	66.0
5	20 Aug.	42.6	40.5	12.9	5.7	50.6	38.7	27.5	10.8	-11.3	29.0	54.4	79.6	17.0	39.3	81.6
6	30 Aug.	16.7	41.1	11.8	18.0	29.7	16.7	40.7	8.4	-16.0	25.4	21.0	77.6	13.7	37.0	60.0
7	8 Sep.	39.4	-3.5	23.6	-20.0	20.5	36.6	-10.4	29.8	1.1	25.6	51.9	27.2	34.0	15.3	38.8
8	14 Sep.	14.2	4.7	14.1	42.4	30.2	13.2	-2.8	11.5	16.2	22.5	18.1	34.1	17.7	78.8	52.2
9	18 Sep.	130.7	-3.4	26.4	-33.3	28.2	135.0	-0.2	50.0	26.4	29.8	175.5	29.8	46.1	16.4	46.0
10	30 Sep.	66.8	54.6	12.7	36.6	27.9	70.0	62.1	9.6	2.8	23.2	83.4	93.1	16.3	75.3	48.0
11	11 Oct.	79.2	-4.3	12.6	5.9	24.7	80.9	-2.3	9.8	-17.4	20.9	98.5	19.0	15.8	32.8	35.3
12	27 Oct.	27.1	37.0	6.9	-23.3	33.1	28.6	44.3	6.8	-24.1	33.7	33.6	69.9	8.9	-1.1	50.8
13	8 Nov.	29.3	46.3	17.8	9.2	31.0	29.1	45.5	17.1	5.0	24.0	37.3	86.0	23.9	46.6	57.6
14	28 Nov.	56.4	45.8	12.6	-8.7	35.9	55.1	42.4	11.2	-19.0	31.8	72.1	86.4	15.6	13.0	63.1
Averages			32.4		18.0	32.4		29.9		12.3	26.1		66.9		37.6	57.5

A comparison of REP, RET and MRE is shown in Fig. 5 for the dynamic wave and kinematic wave methods, in Fig. 6 for the diffusion wave and kinematic wave methods, and in Fig. 7 for the diffusion wave and dynamic wave methods. If the scatter of points are concentrated below the diagonal line rather than above it, the method of the ordinate axis dominates the method of the abscissa axis. It is evident from Fig. 5 and Fig. 6 that the dynamic wave and diffusion wave methods are more accurate than the kinematic wave method, whereas from Fig. 7 it can be seen that the dynamic wave and diffusion wave methods are almost equally accurate in reproducing the observed hydrographs in the case of such a lowland catchment.

Table 5 Comparison of computer time for the three method

Method	For hourly data	For all floods data (248 hours)
Dynamic wave method	4 min. 30 sec.	19 hours
Diffusion wave method	1 min. 30 sec.	4 hours 30 min.
Kinematic wave method	7 sec.	30 min.

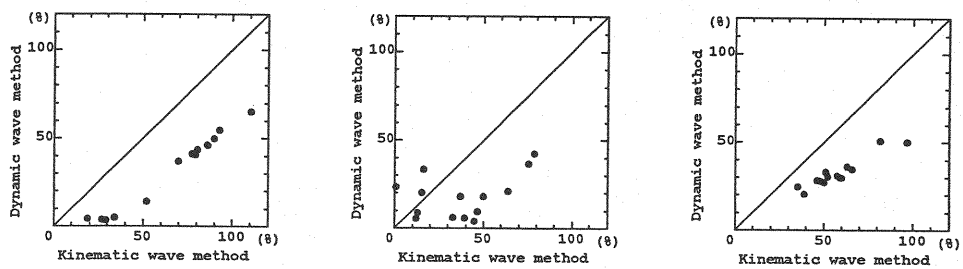

(a) RET (b) REP (c) MRE

Fig. 5 Comparison of the dynamic wave and kinematic wave methods of RET, REP and MRE

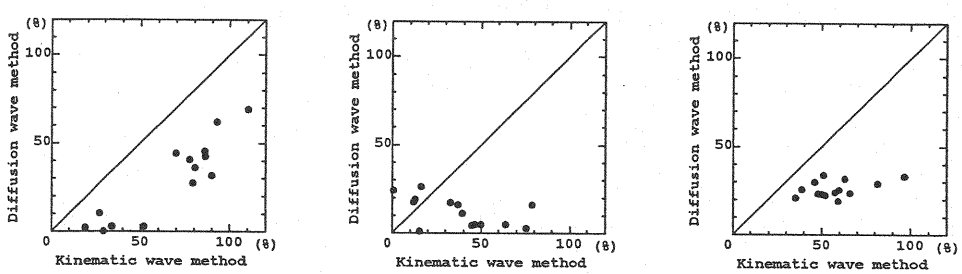

(a) RET (b) REP (c) MRE

Fig. 6 Comparison of the diffusion wave and kinematic wave methods of RET, REP and MRE

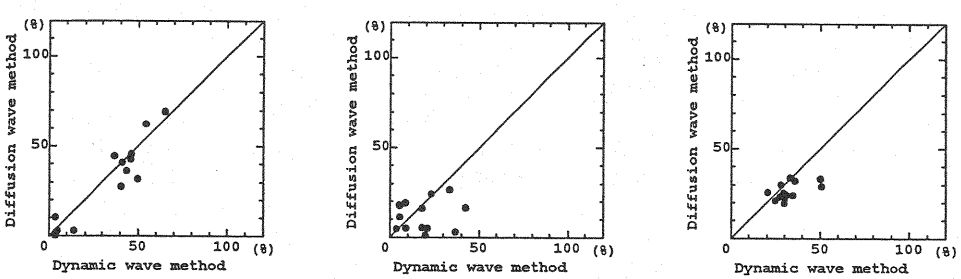

(a) RET (b) REP (c) MRE

Fig. 7 Comparison of the diffusion wave and dynamic wave methods of RET, REP and MRE

CONCLUSION

Three stormwater runoff models based on an effective rainfall model and physical equations are applied to the Shinkomatsu River catchment in an urban lowland area for fourteen rainfall events. The results show that the dynamic wave and diffusion wave methods have approximately equal accuracy in reproducing the observed hydrographs, whereas the kinematic wave method is inaccurate in reproducing the observed hydrographs. Since the diffusion wave method requires less computer time and involves simpler equations, it is the most applicable method for analyzing the stormwater runoff phenomena in this catchment.

REFERENCES

1. Ando, Y. : Relationship between infiltration capacity and topography, soil type and land use in urban area. In: Proc. of Hydraulic Engineering, JSCE, vol.35, pp.123-128, 1991. (in Japanese)
2. Ando, Y., Musiake, K. and Y. Takahasi : Modelling of hydrologic processes in a small urbanized hillslope basin with comments on the effects of urbanization, J. Hydrol. 68, pp.61-83, 1984.
3. Ando, Y., Nabeyama, T. and S. Nishijima : Urban stormwater runoff analysis of upland basins in Tokyo. In: Proc. of the Yokohama Symp. on Hydrology of Warm Humid Regions, IAHS Publ. No.216, pp.403-408, 1993.
4. Ando, Y., Takahasi, Y., Izumi, K. and K. Kanao : Urban flood modeling considering infiltration of various land uses. In: Proc. Int. Symp. on Comparison of Urban Drainage Models with Real Catchment Data: UDM '86, Pergamon Press, Oxford, pp.229-238, 1986.
5. Kadoya, M. : Runoff analysis methods (the sixth report), Jour. JSIDRE, vol.48, No.6, pp.37-43, 1980. (in Japanese)
6. Kinosita, T. : A way for unsteady flow calculation. In: Application of numerical analysis and its basis, Atene Press Inc., Tokyo, pp.143-175, 1971. (in Japanese)
7. Ponce, V.M., Li, R.-M., and D.B. Simons : Applicability of kinematic and diffusion models, J. Hydraul. Div., Proc. ASCE, HY3, pp.353-360, 1978.
8. Richtmyer, R.D. and K.W. Morton : Difference method for initial-value problems, Second edition, Interscience Publishers, a division of John Wiley & Sons, pp.300-311, 1967.
9. Sueishi, T. : On the run-off analysis by the method of characteristics, Hydraulic studies on the run-off phenomena of rain water, 2nd report., Trans. of JSCE., No.29, pp.74-87, 1955. (in Japanese)
10. Tholin, A.L. and C.J. Keifer : The hydrology of urban runoff, Trans. ASCE, vol.125, pp.1308-1379, 1960.
11. Wooding, R.A. : A hydraulic model for the catchment-stream problem, I. Kinematic-wave theory. J. Hydrol. 3, pp.254-267, 1965.
12. Wooding, R.A. : A hydraulic model for the catchment-stream problem, III. Comparison with runoff observations. J. Hydrol. 4, pp.21-37, 1966.
13. Yamaguchi, T., Matsubara, S. and T. Yamamori : Stormwater Runoff from Urban Areas (the second report), Tech. Mem. of Public Works Res. Inst., 14-11, pp.13-39, 1972. (in Japanese)

APPENDIX - NOTATION

The following symbols are used in this paper:

A	= cross-sectional area;
DT	= observed time interval;
g	= gravity constant;
h	= rainwater flow depth on the surface;
H	= channel flow depth;
IC	= final infiltration rate;
k	= number of land use in pervious land use;
K	= channel flow parameter for circular pipe flow;
L	= initial loss of rainfall;
n	= Manning's roughness coefficient;
N	= equivalent roughness;
NM	= number of data;
P	= channel flow parameter for circular pipe flow;
q	= discharge of rainwater flow on the surface;
Q	= channel flow discharge;
QC	= calculated discharge;
QO	= observed discharge;
QPC	= calculated peak discharge;
QPO	= observed peak discharge;
r	= effective rainfall;
R	= hydraulic radius;
R(t)	= rainfall at time t;
Re	= effective rainfall rate;
s, S	= slopes of surface and channel respectively;
t	= time;
Δt	= time interval;
$u = Q/A$	= average flow velocity;
Δx, ΔX	= distance interval respectively; and
x, X	= distance of surface and channel respectively.

Subscripts:

imp	= impervious area; and
p	= pervious area.

(Received June 13, 1996; revised December 2, 1996)